

Production of ^{56}Ni in black hole-neutron star merger accretion disk outflows

R. Surman¹, O.L. Caballero^{2,3}, G.C. McLaughlin⁴, O. Just^{5,6},
H.-Th. Janka⁵

¹Department of Physics and Astronomy, Union College, Schenectady, NY, USA

²Joint Institute for Nuclear Astrophysics, Michigan State University, East Lansing, MI, USA

³Institut für Kernphysik, Technische Universität Darmstadt, Darmstadt, Germany

⁴Department of Physics, North Carolina State University, Raleigh, NC, USA

⁵Max-Planck-Institut für Astrophysik, Garching, Germany

⁶Max-Planck/Princeton Center for Plasma Physics (MPPC)

E-mail: surmanr@union.edu

Abstract. The likely outcome of a compact object merger event is a central black hole surrounded by a rapidly accreting torus of debris. This disk of debris is a rich source of element synthesis, the outcome of which is needed to predict electromagnetic counterparts of individual events and to understand the contribution of mergers to galactic chemical evolution. Here we study disk outflow nucleosynthesis in the context of a two-dimensional, time-dependent black hole-neutron star merger accretion disk model. We use two time snapshots from this model to examine the impact of the evolution of the neutrino fluxes from the disk on the element synthesis. While the neutrino fluxes from the early-time disk snapshot appear to favor neutron-rich outflows, by the late-time snapshot the situation is reversed. As a result we find copious production of ^{56}Ni in the outflows.

Submitted to: *J. Phys. G: Nucl. Phys.*

1. Introduction

Two compact objects (black hole-neutron star or neutron star-neutron star) in a binary system will undergo orbital decay due to gravitational radiation emission and eventually merge. The merger is thought to produce a larger, central compact object surrounded by a rapidly accreting torus of debris. The debris torus may contribute to the energy needed to power a short-duration gamma-ray burst [1, 2, 3, 4]. Some fraction of the mass of the system is expected to be ejected—promptly, in the tidal tails, and in outflows from the accretion disk. Thus merger events are expected to be important contributors to galactic nucleosynthesis. Understanding the nature of this contribution requires accurate predictions of the elemental composition of the ejected material. Additionally, the decay of nuclear species produced in the merger will result in an observable electromagnetic counterpart [5, 6, 7], which will be sensitive to the kinds and amounts of radioactive species produced [8, 9].

The material ejected promptly or in the tidal tails is expected to be cold or only mildly heated and to retain much of the neutron richness of the original neutron star(s). Thus it is an attractive site for the assembly of the heaviest elements in rapid neutron capture, or r-process, nucleosynthesis [10, 11, 12, 7, 13]. The material that makes up the accretion disk outflows, on the other hand, will be highly processed before element synthesis occurs—first in the disk [14], where it is heated and the nuclei dissociated into their constituent nucleons, and then in the outflow [15], where the composition will be set by the weak interactions:



As the accretion disk copiously emits neutrinos [16], the above reverse reactions play a key role in determining the resulting element synthesis in the outflows.

Element synthesis in the hot outflows from merger-type black hole accretion disks has previously been addressed in, e.g., [17, 18, 19, 20, 21, 22]. These found neutron-rich outflows to be possible in this environment, and thus suggested that merger-type disk winds may be an important source of particularly the lighter r-process nuclei. In general neutron-rich outflows may result from two distinct mechanisms: the preservation of the high disk neutron-to-proton ratio in the outflow or the reset of the outflow neutron-to-proton ratio by the neutrino capture reactions from Eqns. 1,2. The latter mechanism is the focus of this work. For the neutrino interactions to drive the outflows neutron-rich, the antineutrinos must be sufficiently hotter than the neutrinos to overcome the neutron-proton mass difference, so that the rate of antineutrino captures on protons can exceed the neutrino capture rate on neutrons. Calculations of disk neutrino decoupling surfaces, similar to protoneutron star (PNS) ‘neutrinospheres’, show that as in the PNS the antineutrinos decouple deeper within the disk and are therefore hotter. However, the decoupling surfaces are not spherical as in the PNS but torus-shaped, so the antineutrinos emerge from a smaller region closer to the black hole. This makes the

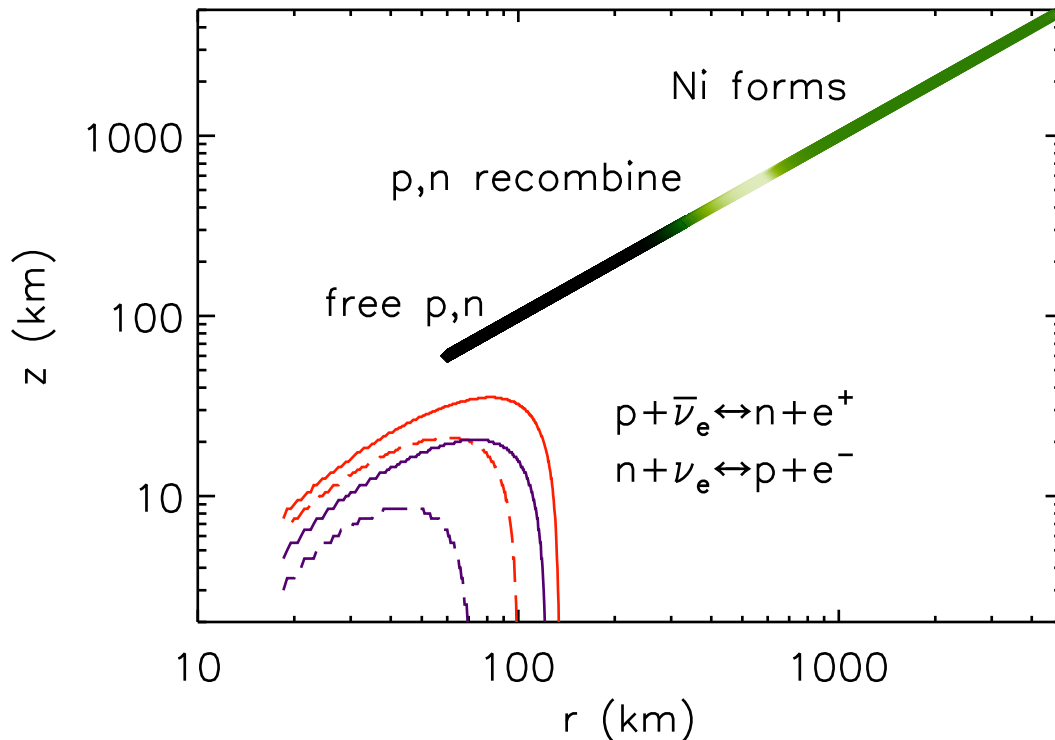


Figure 1. Neutrino (solid) and antineutrino (dashed) decoupling surfaces for the $t=20$ ms (thick red lines) and $t=60$ ms (thin purple lines) disk model snapshots. Also shown is a sample radial outflow trajectory (shaded line), colored according to the mass fraction of alpha particles X_α along the trajectory, where black corresponds to $X_\alpha=0$ and white corresponds to $X_\alpha=1$.

antineutrinos subject to larger general relativistic effects [23] and reduces the expected neutron richness of any neutrino-dominated outflows [24].

Here we address an additional consideration—does the disk neutrino emission persist long enough to make robustly neutron-rich outflows? We consider the nucleosynthesis in the outflows from a time-dependent merger-type black hole accretion disk, carefully incorporating the important general relativistic effects on the neutrino emission from the disk. We find that the mechanism for producing neutron-rich disk outflows via neutrino interactions does not operate in this model. Instead, mildly proton-rich outflows are predicted. We examine the resulting nucleosynthesis and show these outflows can result in significant ^{56}Ni production.

2. Black hole accretion disk model

We begin with a time-dependent model of a merger-type black hole accretion disk. The initial disk model is set up to be the equilibrium configuration of a constant angular momentum torus, similar to [25], where the black hole has a mass of 3 solar

masses and spin parameter of $a = 0.8$. The simulated physics are Newtonian, except for the gravitational potential, which is given by the pseudo-relativistic Artemova-Novikov-Bjoernsson potential [26]. The equation of state takes into account non-relativistic baryons (neutrons, protons, alphas, and one heavy nucleus), relativistic and/or degenerate electrons, and a plasma, and is similar to [27]. At $t = 0$ s the Shakura and Sunyaev alpha viscosity terms are turned on and the subsequent disk dynamics are followed.

We take two time snapshots of this accretion disk model, at $t = 20$ ms and $t = 60$ ms, for careful study. The first time snapshot is representative of the disk just after formation and corresponds to conditions similar to those from, for example, [20]. We consider outflows launched from this disk at $t = 20$ ms. As the outflowing material moves away from the disk, it will continue to be affected by the neutrino emission from the evolving disk. Thus, we use a second disk snapshot to capture the general behavior of the time evolution of the disk neutrino emission. The neutrino interactions are the most important during the early part of the outflow, within the first tens of milliseconds from launch, so we choose $t = 60$ ms for the second snapshot. For each disk snapshot, we calculate the electron neutrino and antineutrino decoupling surfaces as in [23] and take the neutrino emission to be thermal, with a temperature equal to the local disk temperature at the point of decoupling. The neutrino decoupling surfaces for the two disk snapshots are shown in Fig. 1. At early times, both the electron neutrino and antineutrino decoupling surfaces are large, and the antineutrinos emerge from deeper within the disk and are therefore hotter. By $t = 60$ ms, the disk has already lost enough mass to substantively change its structure—neutrino emission drops and the neutrino decoupling surfaces shrink. These changes to the neutrino emitting regions will strongly impact the resulting nucleosynthesis in the outflows.

3. Neutrino interactions in the outflow

To study the nucleosynthesis produced in hot outflows from this disk, we use an outflow model based on a streamline approach. We construct the model by first constraining the outflow to follow radial streamlines with zero vorticity. We use the steady flow approximation and consider the Bernoulli function along the streamline that defines the outflow trajectory. In its simplest form, the Bernoulli function is

$$B = \frac{1}{2}v^2 + h + \Phi, \quad (3)$$

where v is the outflow velocity, h is the specific enthalpy, and $\Phi = -GM_{BH}/r$ is the gravitational potential with M_{BH} the black hole mass, r the distance to the black hole of a mass element, and G the gravitational constant. We write the specific enthalpy as

$$h = \frac{1}{\rho} \left[\sum_i n_i \mu_i + (kT)(s/k)n_B \right], \quad (4)$$

where ρ is the density, T is the temperature, n_B is the baryon number density, and n_i and μ_i are the number density and chemical potential, respectively, of species i , where the

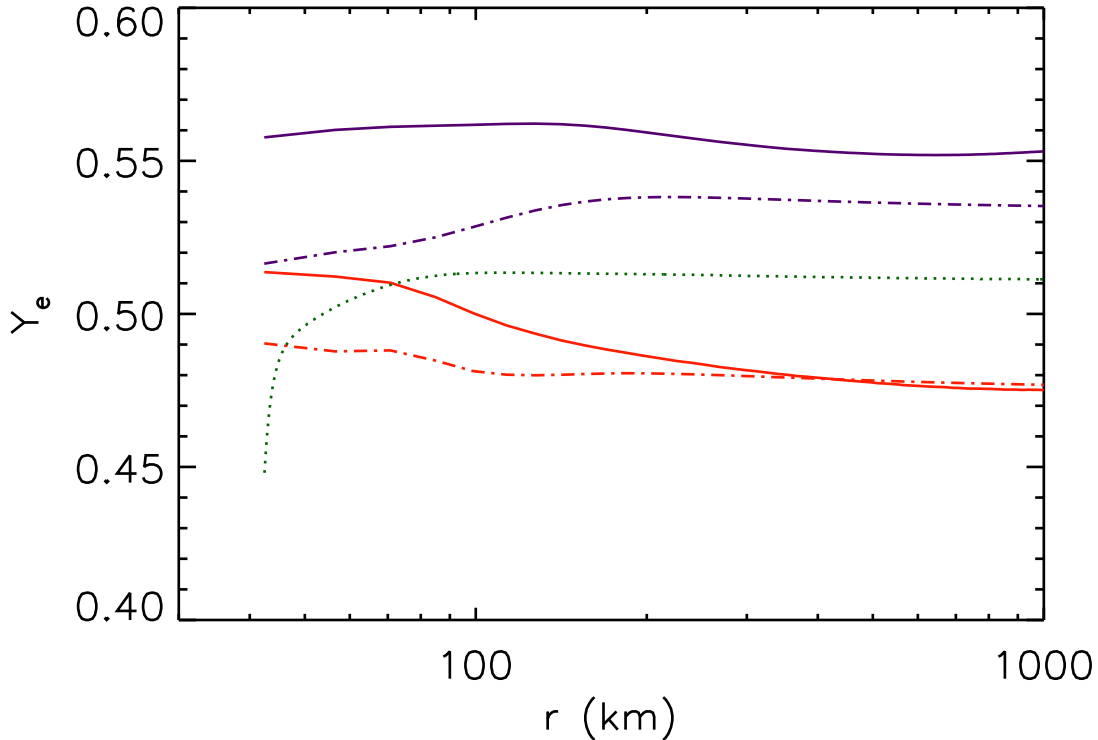


Figure 2. Neutrino-only equilibrium electron fractions $Y_e^{\nu\text{-only eq}} = 1/(1 + \lambda_{\bar{\nu}_e p}/\lambda_{\nu_e n})$ along a sample radial outflow trajectory for the $t = 20$ ms (thick red lines) and the $t = 60$ ms (thin purple lines) disk model snapshots, with (solid) and without (dot-dashed) GR effects on the neutrino fluxes. The outflow electron fractions obtained in the full calculation, starting from the disk value of 0.446, tend to fall in between, as shown here for a $s/k = 30$, $\tau = 10$ ms outflow trajectory (dotted line).

sum over species includes electrons, positrons, neutrons, protons, alpha particles, and an average heavy nucleus [28, 29]. We solve for the outflow hydrodynamics by further assuming a constant mass outflow rate, $\dot{M} = 4\pi r^2 \rho v$, which remains a free parameter in this formulation. As in [30], we choose to follow adiabatic trajectories and take the Bernoulli function to be constant along the streamline. The resulting trajectories, parameterized in entropy and mass outflow rate, are qualitatively similar to standard supernova neutrino-driven wind trajectories [31], parameterized in entropy and dynamic timescale τ , where $r \sim r_0 e^{t/\tau}$, so we adopt the latter prescription.

We launch material from the inner region of the disk, at $t = 20$ ms and $r_0 = 30$ km; a schematic of the trajectory is given in Fig. 1. We take the starting composition of the outflow to be the local $t = 20$ ms disk composition at that point, which is a mix of neutrons and protons with an electron fraction $Y_e = 1/(1 + n/p)$ of 0.446. We then evolve the composition, taking careful account of the weak reactions Eqns. 1,2 throughout.

Of particular importance are the neutrino capture reactions on nucleons, Eqns. 1,2. The rates of these reactions, $\lambda_{\nu_e n}$ and $\lambda_{\bar{\nu}_e p}$, respectively, are given by

$$\lambda_{\nu_e n} = b \int_0^\infty \phi_\nu^{\text{eff}}(E + \Delta)^2 \sqrt{1 - \left(\frac{m_e}{E + \Delta}\right)^2} W_M dE \quad (5)$$

$$\lambda_{\bar{\nu}_e p} = b \int_{\Delta + m_e c^2}^\infty \phi_{\bar{\nu}}^{\text{eff}}(E - \Delta)^2 \sqrt{1 - \left(\frac{m_e}{E + \Delta}\right)^2} W_{\bar{M}} dE, \quad (6)$$

where $b = 9.704 \times 10^{-50} \text{ cm}^2 \cdot \text{keV}^{-2}$, m_e is the electron mass, Δ is the neutron-proton mass difference, $W_M = 1 + 1.1(E/m_n)$ and $W_{\bar{M}} = 1 - 7.1(E/m_n)$ are the weak magnetism corrections [33] and ϕ_ν^{eff} , $\phi_{\bar{\nu}}^{\text{eff}}$ are the effective neutrino and antineutrino fluxes in units of $1/(\text{cm}^2 \cdot \text{s} \cdot \text{keV})$. The effective neutrino and antineutrino fluxes as observed by the outflowing fluid element above each disk snapshot are calculated as in [24]. We integrate the thermal fluxes described in Sec. 2 above over the solid angle of the emitting surface, both with and without general relativistic (GR) corrections to the neutrino energies and trajectories. The neutrino and antineutrino capture rates are then calculated from each set of these fluxes along the radial outflow path.

To get a sense of what type of nucleosynthesis we can expect as well as the impact of the GR effects and the time-dependence of the neutrino fluxes, we examine the neutrino-only equilibrium electron fraction along the radial outflow path, calculated separately for the $t = 20$ ms and $t = 60$ ms disk snapshots. The neutrino-only equilibrium electron fraction, $Y_e^{\nu\text{-only eq}}$, is the composition that would be expected if the neutrino interaction rates are much greater than the reverse weak rates of electron/positron capture, and is calculated by $Y_e^{\nu\text{-only eq}} = 1/(1 + \lambda_{\bar{\nu}_e p}/\lambda_{\nu_e n})$. The results are shown in Fig. 2. We can see that if the $t = 20$ ms disk snapshot were taken to be steady-state and the GR effects on the neutrino spectra are ignored, the outflows would tend to be driven neutron rich by neutrino interactions. However, once the GR effects are included, the situation changes, as first pointed out in [24]. The antineutrinos come from a smaller emitting surface closer to the black hole than the neutrinos, and so the antineutrino fluxes are more strongly shaped by the GR effects, particularly the redshifting of the neutrino energies. Thus at the start of the trajectory the strong neutron-richness predicted in the no-GR $Y_e^{\nu\text{-only eq}}$ is lost. By $t = 60$ ms, the antineutrino emitting surface has become so small that, even though the antineutrinos are still hotter than the neutrinos, the material along the outflow trajectory ‘sees’ more neutrinos than antineutrinos, and $\lambda_{\nu_e n} > \lambda_{\bar{\nu}_e p}$ and $Y_e^{\nu\text{-only eq}} > 0.5$.

The effects of the time dependence of the neutrino fluxes are estimated by a simple linear scheme. The outflow is launched at $t = 20$ ms, and from $t = 20$ ms to $t = 60$ ms the neutrino capture rates are taken to be

$$\lambda(t) = \lambda^{t=20 \text{ ms}} + \left(\frac{t - 20 \text{ ms}}{40 \text{ ms}}\right) (\lambda^{t=60 \text{ ms}} - \lambda^{t=20 \text{ ms}}) \quad (7)$$

and for $t > 60$ ms $\lambda(t) = \lambda^{t=60 \text{ ms}}$, where $\lambda^{t=20 \text{ ms}}$ and $\lambda^{t=60 \text{ ms}}$ are the interaction rates calculated with the $t = 20$ ms and $t = 60$ ms disk neutrino fluxes, respectively. This choice of an interpolation scheme captures the general features of the time dependence of

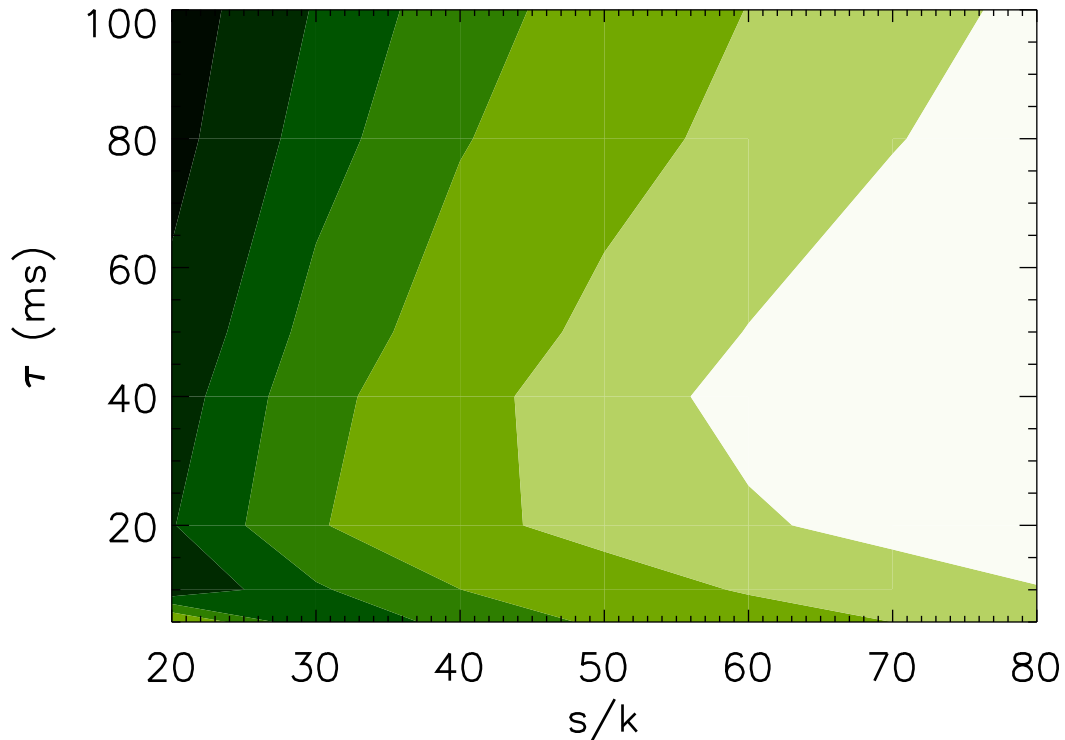


Figure 3. Nickel-56 production for the outflow parameter space—entropy per baryon s/k and effective dynamic timescale τ —sampled in this work. The shaded regions correspond to nickel mass fractions of 0.5, 0.4, 0.3, 0.2, 0.1, and less than 0.1, from darkest to lightest.

the neutrino fluxes and should influence only the details of the predicted nucleosynthetic yields and not the general conclusions.

4. Element synthesis

Using the neutrino interaction rates described above, we follow the element synthesis as in [30], first with an NSE calculation [29] and then switching over to a full nuclear network [32] at $T = 10$ GK. We examine a range of our outflow parameter space: entropies $20 \leq s/k \leq 80$ and effective dynamic timescales $10 \text{ ms} \leq \tau \leq 100 \text{ ms}$. As anticipated, the actual evolution of the electron fraction in the outflow tends to lie somewhere in between the $Y_e^{\nu\text{-only eq}}$ values for the two disk snapshots, as shown for an example full trajectory in Fig. 2. As a result, we find proton-rich nucleosynthesis products in almost all of the outflows studied.

The nucleus with $A > 4$ most vigorously produced is ^{56}Ni . The final mass fractions of nickel in the outflows are shown in Fig. 3. For mildly heated outflow material over half is ejected as ^{56}Ni . Increases in heating tend to favor lighter nuclei, and so for trajectories with higher entropy most of the material is left as alpha particles. Still, ^{56}Ni remains

the most abundantly produced $A > 4$ nucleus.

Note that the prediction of nickel-rich outflows for this disk model depends strongly on the neutrino physics and is largely insensitive to the particular outflow parameterization chosen. We draw the same conclusions regarding ^{56}Ni production when we repeat the nucleosynthesis calculations using the outflow model from [18].

5. Conclusion

Merger-type black hole accretion disks have been shown to be attractive potential sites for neutron-rich nucleosynthesis. Here we examine one potential mechanism for producing neutron-rich outflows—via neutrino interactions in the outflow—and note that its operation is not ubiquitous. In our calculations, we find that the combination of general relativistic effects on the neutrino fluxes as well as the rapid evolution of the neutrino emission surfaces have the opposite effect. The resulting proton-rich outflows will not produce r-process nuclei but may be a rich source of ^{56}Ni .

Any ^{56}Ni produced will decay first into ^{56}Co then ^{56}Fe . Such decays power the light curves of core-collapse supernovae and so could potentially produce an observable electromagnetic counterpart to the merger event. If $\sim 1\%$ of the disk mass is ejected in winds that are driven proton-rich by the neutrino physics, on the order of $10^{-3}M_{\odot}$ of ^{56}Ni may be ejected. This is sufficient to generate a bright optical peak [8], which would be in addition to the infrared peak expected to be due to the radioactive r-process ejecta [5, 6, 7].

Acknowledgments

This work was supported by the Department of Energy under contracts DE-FG02-05ER41398 (RS) and DE-FG02-02ER41216 (GCM). OJ and TJ acknowledge support by the Computational Center for Particle and Astrophysics (C2PAP) as part of the Cluster of Excellence EXC 153 “Origin and Structure of the Universe” and by the Max-Planck-Princeton Center for Plasma Physics.

References

- [1] Paczyński B 1986 *Astrophys. J.* 308 L43
- [2] Eichler D, Livio M, Piran T, and Schramm D 1989 *Nature* 340 126
- [3] Janka H-Th, Eberl T, Ruffert M, and Fryer CL 1999 *Astrophys. J.* 527 L39
- [4] Rosswog S and Liebendoerfer M 2003 *Monthly Notices Royal Astron. Soc.* 342 673
- [5] Metzger B D, et al. 2010 *Monthly Notices Royal Astron. Soc.* 406 2650
- [6] Roberts L F, Kasen D, Lee W H, and Ramirez-Ruiz E 2011 *Astrophys. J.* 736, L21
- [7] Goriely S, Bauswein A, and Janka H-Th 2011 *Astrophys. J.* 738 L32
- [8] Barnes J and Kasen D 2013 *Astrophys. J.* 775 18
- [9] Grossman D, Korobkin O, Rosswog S, and Piran T 2013, submitted to *Monthly Notices Royal Astron. Soc.*, [arXiv:1307.2943]
- [10] Lattimer J M and Schramm D N 1974 *Astrophys. J.* 192 L145

- [11] Meyer B S 1989 *Astrophys. J.* 343 254
- [12] Freiburghaus C, Rosswog S, and Thielemann F-K 1999 *Astrophys. J.* 525 L121
- [13] Korobkin O, Rosswog S, Arcones A, and Winteler C 2012 *Monthly Notices Royal Astron. Soc.* 426 1940
- [14] Surman R and McLaughlin G C 2004 *Astrophys. J.* 603 611
- [15] Surman R and McLaughlin G C 2004 *Astrophys. J.* 618 397
- [16] McLaughlin G C and Surman R 2007 *Phys. Rev. D* 75 023005
- [17] McLaughlin G C and Surman R 2005 *Nucl. Phys. A* 758 189
- [18] Surman R, McLaughlin G C, and Hix W R 2006 *Astrophys. J.* 643 155
- [19] Metzger B D, Thompson T A, and Quataert, E 2008 *Astrophys. J.* 676 1130
- [20] Surman R, McLaughlin G C, Ruffert M, Janka H-Th, and Hix W R 2008 *Astrophys. J.* 679 L117
- [21] Wanajo S Y and Janka H-Th 2012 *Astrophys. J.* 746 180
- [22] Rosswog S, Korobkin O, Arcones A, and Thielemann F-K 2013, submitted to Monthly Notices Royal Astron. Soc. [arXiv:1307.2939]
- [23] Caballero O L, McLaughlin G C, and Surman R 2009 *Phys. Rev. D* 80 123004
- [24] Caballero O L, McLaughlin G C, and Surman R 2012 *Astrophys. J.* 745 170
- [25] Iugumenshchev I V, Chen X, and Abramowicz M A 1996 *Monthly Notices Royal Astron. Soc.* 278 236
- [26] Arternova I V, Bjoernsson G, and Novikov I D 1996 *Astrophys. J.* 461 565
- [27] Timmes F X and Swesty F D 2000 *Astrophys. J. Suppl. Ser.* 126 501
- [28] Lattimer J M and Swesty F D 1991 *Nucl. Phys. A* 535, 331
- [29] McLaughlin G C, Fuller G M, and Wilson J R 1996 *Astrophys. J.* 472 440
- [30] Surman R, McLaughlin G C, and Sabbatino N 2011 *Astrophys. J.* 743 155
- [31] Qian Y-Z and Woosley S E 1996 *Astrophys. J.* 471 331
- [32] Hix W R and Thielemann F-K 1999 *J. Comput. Appl. Math.* 109 321
- [33] Horowitz C J 2002 *Phys. Rev. D* 65 043001